Electronic Supporting Information for

Ruthenium Bisoxazoline Complex as Photoredox Catalyst for Nitro Compound Reduction under Visible Light

Wei-Guo Jia*[a], Ming-Xia Cheng[a], Li-Li Gao[a], Siu Min Tan,[b] Chao Wang,[b] Xiaogang Liu,[b] Richmond Lee*[b]

a: The Key Laboratory of Functional Molecular Solids, Ministry of Education, Anhui Laboratory of Molecular-Based Materials (State Key Laboratory Cultivation Base), College of Chemistry and Materials Science, Anhui Normal University, Wuhu, 241002, China E-mail: wgjiasy@mail.ahnu.edu.cn.

b: Science and Mathematics Cluster, Singapore University of Technology and Design, 8 Somapah Rd Singapore 487372 E-mail: richmond_lee@sutd.edu.sg.

EXPERIMENTAL SECTION

Materials and measurements.

All the operations were carried out under a pure nitrogen atmosphere using standard Schlenk techniques. All solvents were purified and degassed by standard procedures. $[Ru(DMOX)_2Cl_2]$ was synthesized according to literature methods.[1] ^1H and ^{13}C NMR were recorded on a Bruker AV 400/500 MHz NMR spectrometer at room temperature. Chemical shifts (δ) are given in ppm relative to internal TMS and are internally referenced to residual ^1H and ^{13}C solvent resonances. IR spectra were recorded on a Niclolet AVATAR-360IR spectrometer Mass spectra were obtained with MicroTof (Bruker Daltonics, Bremen, Germany) spectrometers. The excitation and emission spectra as well as the lifetime of ccomplex **1** were measured with Edinburgh Instruments (FLS1000). Cyclic voltammetry and differential pulse voltammetry (DPV) measurements were performed on a CHI 650C electrochemical workstation (Shanghai Chenhua Instruments Co., China). A standard three-electrode setup with platinum wire auxiliary electrode, glass carbon working electrode, and Ag/AgCl as the reference electrode. All potentials given in this work are referenced to the Ag/AgCl. For studies performed in tetrabutylammonium hexafluorophosphate (0.1 M) as supporting electrolyte at scan rate of 100 $mV.s^{-1}$. Color temperature of white LED is 6500K, and emission spectra is 455 nm; the commercial supplier: Zhongshan pinuo optoelectronic technology Co. LTD. (website: https://shop116918486.taobao.com/?spm=a1z10.1-c.0.0.275b5697NBZGPA.

Synthesis of Bis(4,4,4',4'-tetramethyl-2,2'-bisoxazoline)(2,2'-bipyridine) ruthenium(II) hexafluorophosphate complex $[Ru(DMOX)_2(Bpy)](PF_6)_2$ (1)

Dichlorobis(4,4,4',4'-tetramethyl-2,2'-bisoxazoline)ruthenium (II) 0.1129 g (0.2 mmol) and 2,2'-bipyridine 0.0344 g (0.22 mmol) were suspended in ethylene glocol (8 mL) in 25 mL schlenk tube and heated at 160 °C for 6 h. The resulting solution was poured into excess aqueous KPF_6 (15 mL), and the thick orange precipitate was obtained by filtration and washed with water (5 mL × 3) and ethyl ether (5 mL ×3). The solid was dissolved in acetonitrile, filtrated and removed under reduced pressure to give **1** as an orange red solid, dried in a vacuum. Yield: 90% (0.1693 g). ^1H NMR (500 MHz, DMSO-d_6, ppm): δ = 8.86 (d, J = 5.0 Hz, 2H), 8.77 (d, J = 15.0 Hz, 2 H), 8.21 (t, J = 10.0 Hz, 2 H), 7.68 (d, J = 10.0 Hz, 2 H), 4.92 (d, J = 10.0 Hz, 2 H), 4.71 (d, J = 15.0 Hz, 2 H), 4.59 (s, 4 H), 1.68 (s, 6 H), 1.15 (s, 6 H), 0.80 (s, 6 H), 0.11 (s, 6 H).^{13}C NMR (125 MHz, DMSO-d_6, ppm): δ = 159.7, 159.6, 157.8, 138.9, 128.0, 124.2, 83.6, 83.5, 71.4, 71.2, 28.1, 26.9, 25.8, 25.5. ESI-MS (positive ions) for $[C_{30}H_{40}N_6O_4Ru]^{2+}$: m/z 325.1079 (calcd for $[M-2PF_6]^{2+}$ 325.1076),

$[C_{30}H_{40}N_6O_4Ru]^+$: m/z 795.1702 (calcd for $[M-PF_6]^+$ 795.1799). IR (KBr cm^{-1}): 3450 (b), 2980 (m), 2941 (m), 2901 (m), 2280 (m), 1647 (m), 1501 (s), 1462 (m), 1371 (m), 1361 (m), 1345 (m), 1267 (m), 1206 (m), 1168 (m), 1025 (m), 991 (m), 936 (m), 844 (s), 628 (m), 559 (m).

General procedure for the reduction of nitroarenes to anilines with the ruthenium photocatalysts The ruthenium complex (0.006 mmol, 0.02 equiv) was dissolved in ACN : EtOH = 1 :19 (6.0 mL), then appropriate nitroarene (0.3 mmol, 1.0 equiv) and $NaBH_4$ (3 mmol, 10 equiv) was added. Subsequently, the resulting mixture was irradiated with 36 W white LEDs from a distance of ca. 5 cm and stired for 3 h at room temperature. After completion of the reaction (monitored by GC), solvents were removed in vacuo from combined organic extracts, the crude products loaded directly onto a column of silica gel and purified by column chromatography to yield the corresponding products.

X-ray Structure Determination. Diffraction data of **1** was collected on a Bruker AXS SMART APEX diffractometer, equipped with a CCD area detector using Mo Kα radiation (λ = 0.71073 Å). All the data were collected at 298K and the structures were solved by direct methods and subsequently refined on F^2 by using full-matrix least-squares techniques (SHELXL),[2] SADABS[3] absorption corrections were applied to the data, all non-hydrogen atoms were refined anisotropically, and hydrogen atoms were located at calculated positions. All calculation was performed using the Bruker Smart program.

References

1. A. Srikanth, G. Nagendrappa and S. Chandrasekaran, *Tetrahedron*, 2003, 59, 7761-7765.
2. Sheldrick, G., SHELXL-97, a program for refining crystal structures. *University of Göttingen, Germany* **1997**.
3. Sheldrick, G., SADABS v. 2.01, Bruker/Siemens area detector absorption correction program. *Bruker AXS, Madison, WI, USA* **1998**.

Table S1. Crystallographic Data and Structure Refinement Parameters for Ruthenium complex

	1
Empirical formula	$C_{30}H_{40}F_{12}N_6O_4P_2Ru$
Formula weight	939.69
Crystal system	monoclinic
Space group	P121/n1
a(Å)	10.8673(4)
b (Å)	27.2041(9)
c (Å)	13.2100(5)
β (°)	104.0360(10)
Volume (Å^3), Z	3788.7(2),4
D_c (mg / m^3)	1.647
μ (Mo-Kα) (mm^{-1})	0.601
F(000)	1904
θ range (°)	2.963 ~ 27.538
Limiting indices	-14, 14; -35, 35; -17, 17
Reflections/unique[R(int)]	8657 / 7341 [0.0350]
Completeness to θ (°)	27.538 (99 %)
Data/restraints/parameters	8657/757/540
Goodness-of-fit on F^2	1.136
R_1, wR_2 [$I > 2s(I)$][a]	R_1 = 0.0540, wR_2 = 0.1189
R_1, wR_2 (all data)	R_1= 0.0673, wR_2 = 0.1249

[a] $R_1 = \Sigma||F_o|-|F_c||/\Sigma|F_o|$; $wR_2 = [\Sigma w(|F_o^2|-|F_c^2|)^2/\Sigma w|F_o^2|^2]^{1/2}$.

Table S2. Selected bond lengths (Å) and bond angels (°) for ruthenium complex

	1
Ru1-N1	2.157(3)
Ru1-N2	2.110(3)
Ru1-N3	2.150(3)
Ru1-N4	2.108(3)
Ru1-N5	2.051(3)
Ru1-N6	2.042(3)
N1-Ru1-N2	77.16(11)
N1-Ru1-N3	85.65(12)
N1-Ru1-N4	97.40(11)
N1-Ru1-N5	174.19(12)
N1-Ru1-N6	99.15(12)
N2-Ru1-N3	98.99(13)
N2-Ru1-N4	173.76(12)
N2-Ru1-N5	97.12(12)
N2-Ru1-N6	88.78(13)
N3-Ru1-N4	77.35(12)
N3-Ru1-N5	96.36(12)
N3-Ru1-N6	171.64(13)
N4-Ru1-N5	88.37(12)
N4-Ru1-N6	95.17(12)
N5-Ru1-N6	79.53(13)

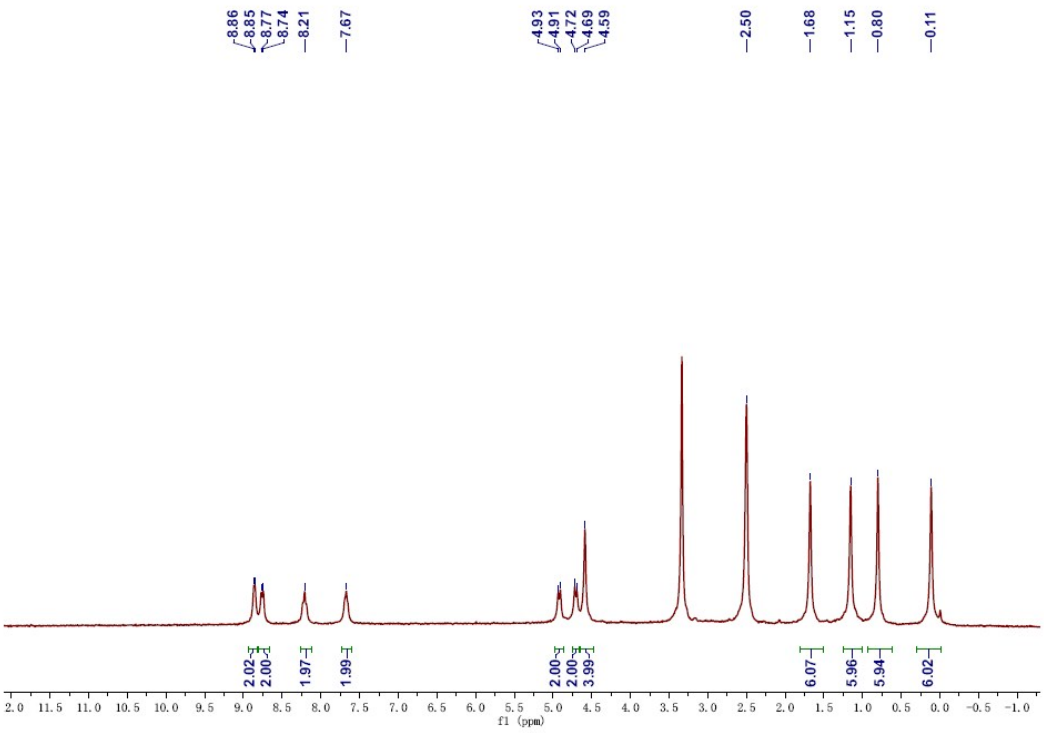

Figure S1. The ^{1}H NMR of **1** (500 MHz, DMSO-d_6)

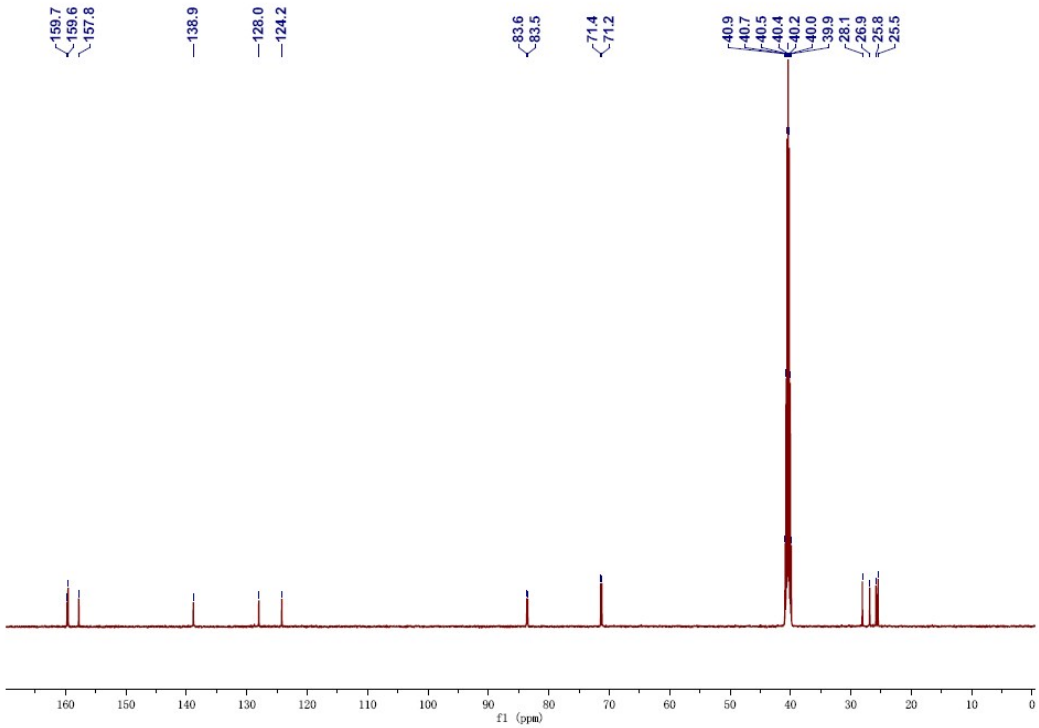

Figure S2. The ^{13}C NMR of **1** (125 MHz, DMSO-d_6)

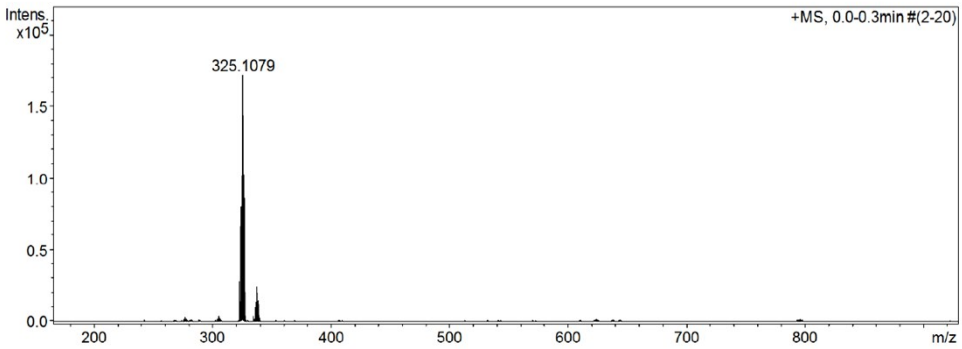

(a)

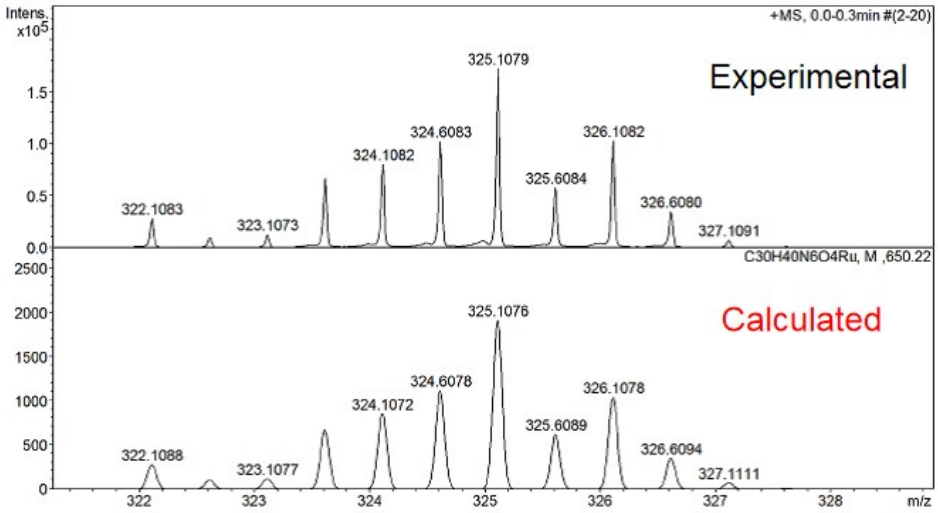

(b)

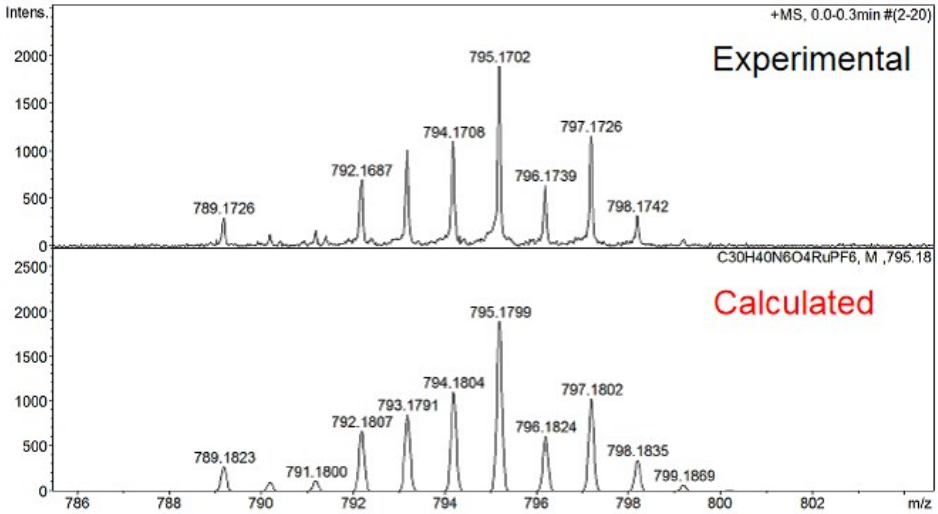

(c)

Figure S3. (a) The ESI-MS spectra of complex **1** with full range**; (b), (c)** Calculated and experiment MS spectra for $[M\text{-}2PF_6]^{2+}$ and $[M\text{-}PF_6]^{+}$

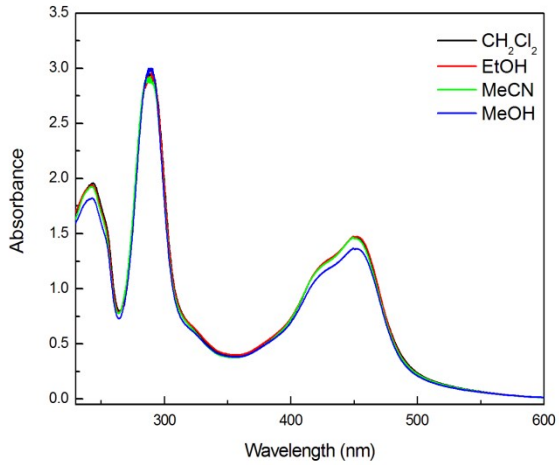

Fig. S4 The absorption of the complex **1** (2×10^{-5} mol/L) in different solvents at room temperature. (maxima: 451 nm, extinctions coefficient: 1.456×10^{4} L mol^{-1} cm^{-1} (CH_2Cl_2; EtOH and MeCN), 1.362×10^{4} L mol^{-1} cm^{-1} (MeOH))

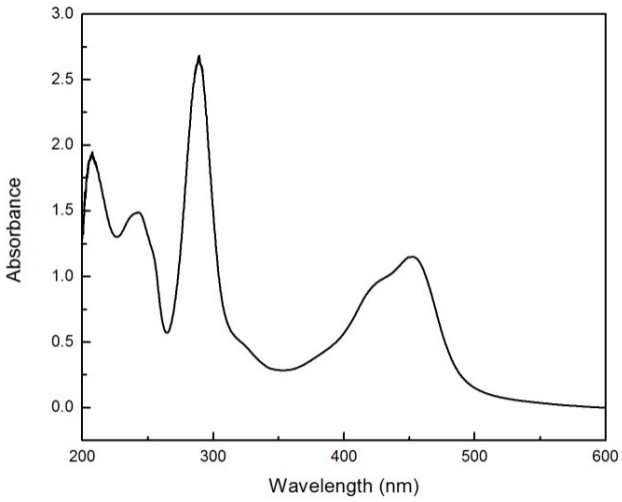

Fig. S5 The absorption of the complex **1** (1×10^{-4} mol/L) in MeCN/EtOH (v/v = 1:19) at room temperature. (maxima: 451 nm, extinctions coefficient: 1.146×10^{4} L mol^{-1} cm^{-1})

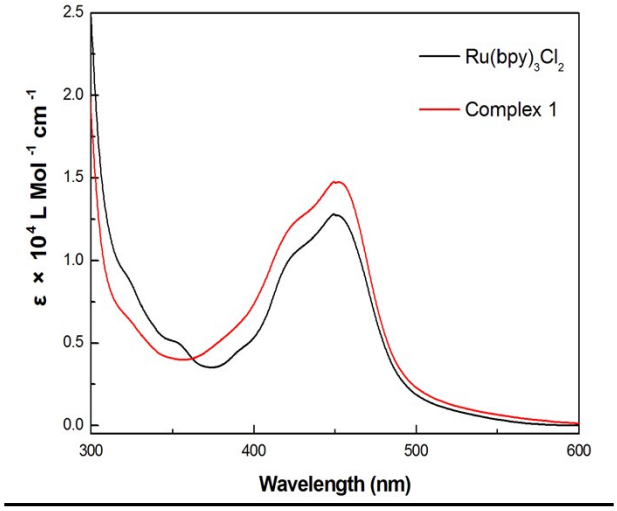

Fig. S6 The absorption of the complex **1** and $Ru(bpy)_3Cl_2$ in MeCN/EtOH (v/v = 1:19 10^{-4} M) at room temperature. (maxima: 451 nm, extinctions coefficient: 1.471×10^4 L mol^{-1} cm^{-1} for complex **1** and 1.279×10^4 L mol^{-1} cm^{-1} for $Ru(bpy)_3Cl_2$)

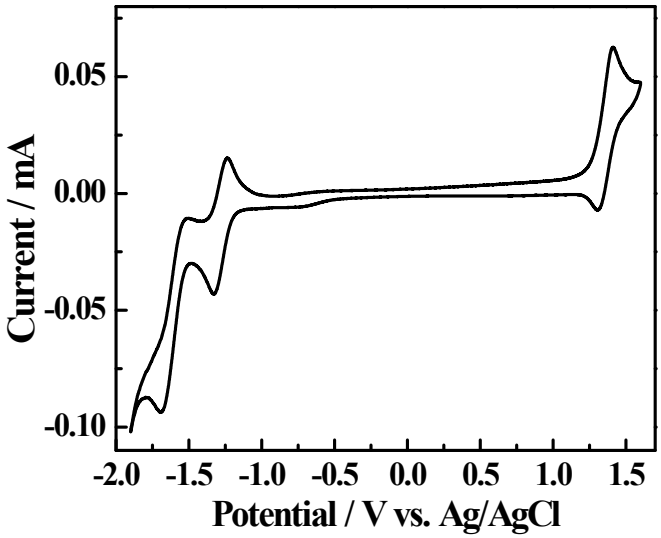

Fig. S7 Cyclic voltammogram of the complex **1** at the potential window of -1.9-1.6 V in dry solvent (MeCN:EtOH = 1:2, 2×10^{-3} M), using tetra-butylammonium hexafluorophosphate (0.1 M) as supporting electrolyte at the scan rate of 100 mV s^{-1}.

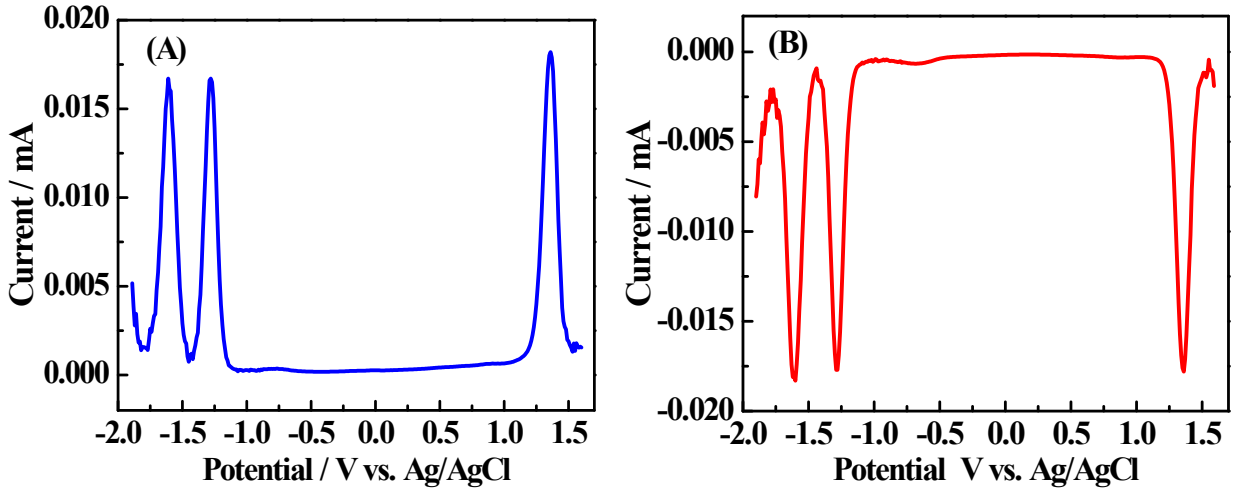

Fig. S8 Differential pulse voltammogram of the complex **1** in the positive potential direction from -1.9 to 1.6 V (A) and the negative potential direction from 1.6 to -1.9 V (B), using tetra-butylammonium hexafluorophosphate (0.1 M) as supporting electrolyte in dry solvent (MeCN:EtOH = 1:2, 2×10^{-3} M). Modulation amplitude: 0.02 V, pulse width: 0.06 s, sample width: 0.02 s.

Table S3. Photophysical and electrochemical properties of complex 1 and $Ru(bpy)_3Cl_2$

	Absorption λ_{max} nm	Emission λ_{max} nm	φ, %	τ, ns	$E_{1/2}$ (Ox), V	$E_{1/2}$ (Red), V
$Ru(bpy)_3Cl_2$	244,288, 435,450	613	5	821	1.05	-1.64, -1.87, -1.99
Complex **1**	238,287,451	610	0.6	155	1.36	-1.60, -1.29

Reference: C. E. Hauke, A. N. Oldacre, C. R. P. Fulong, A. E. Friedman and T. R. Cook, *Inorg. Chem.*, 2018, **57**, 3587-3595.

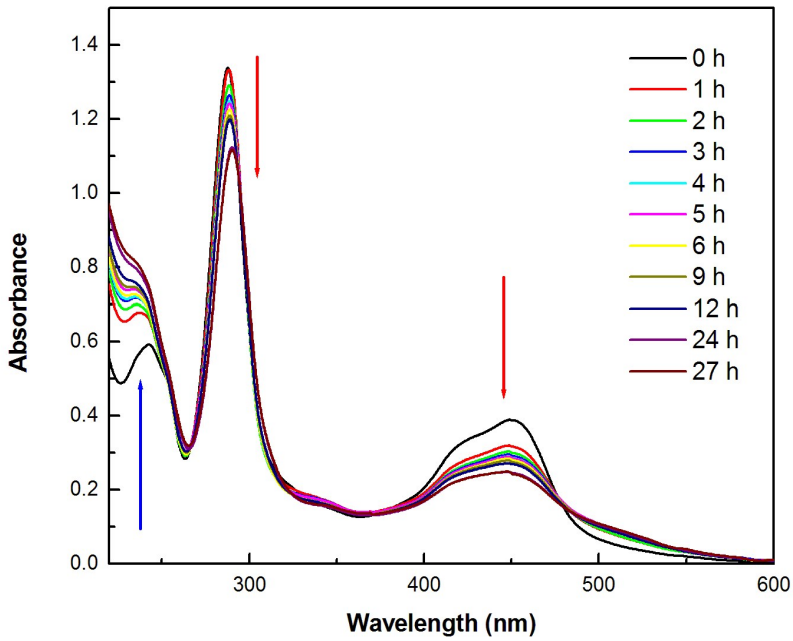

Fig. S9 UV-visible absorption monitoring of the stability of complex **1** under the irradiation with 36 W white LED. Spectrum recorded at ambient temperature in solvent (MeCN:EtOH=1:19, 2×10^{-5} M).

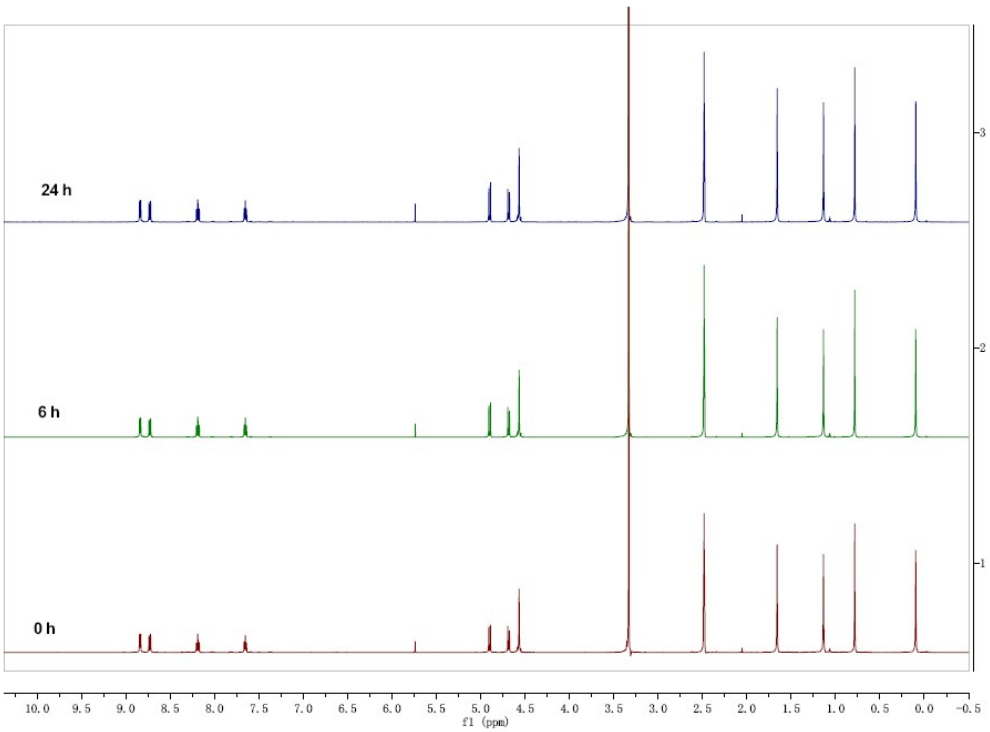

Fig. S10 ^{1}H NMR monitoring of the stability of complex **1** in DMSO-d_6 in the dark at ambient temperature.

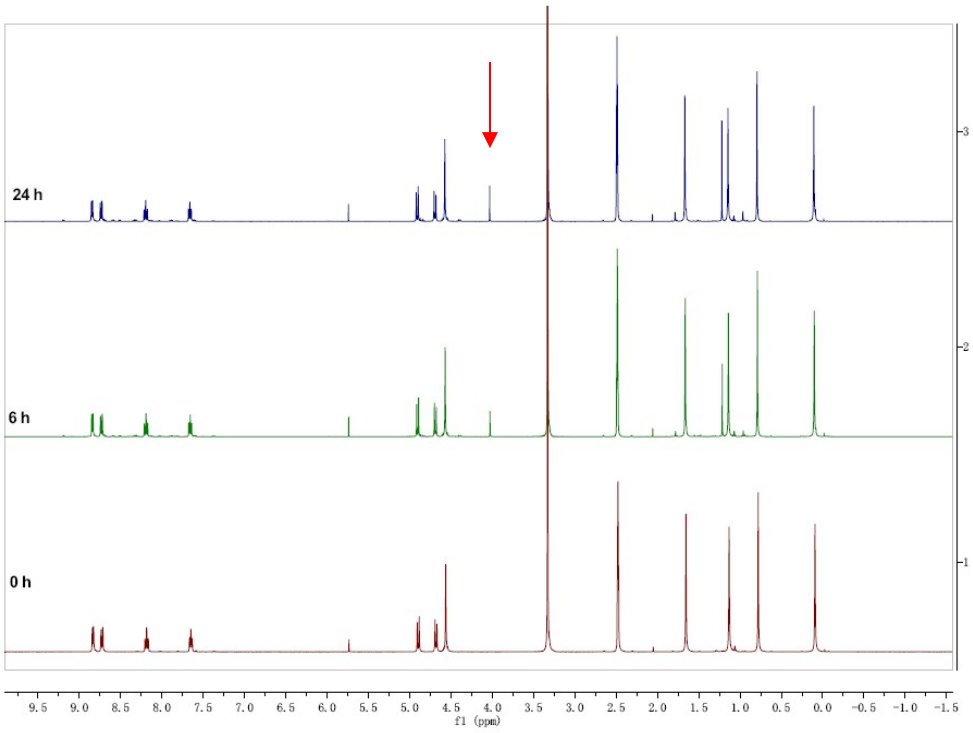

Fig. S11 ^{1}H NMR monitoring of the stability of complex **1** in DMSO-d_6 under irradiated with 36 W white LEDs.

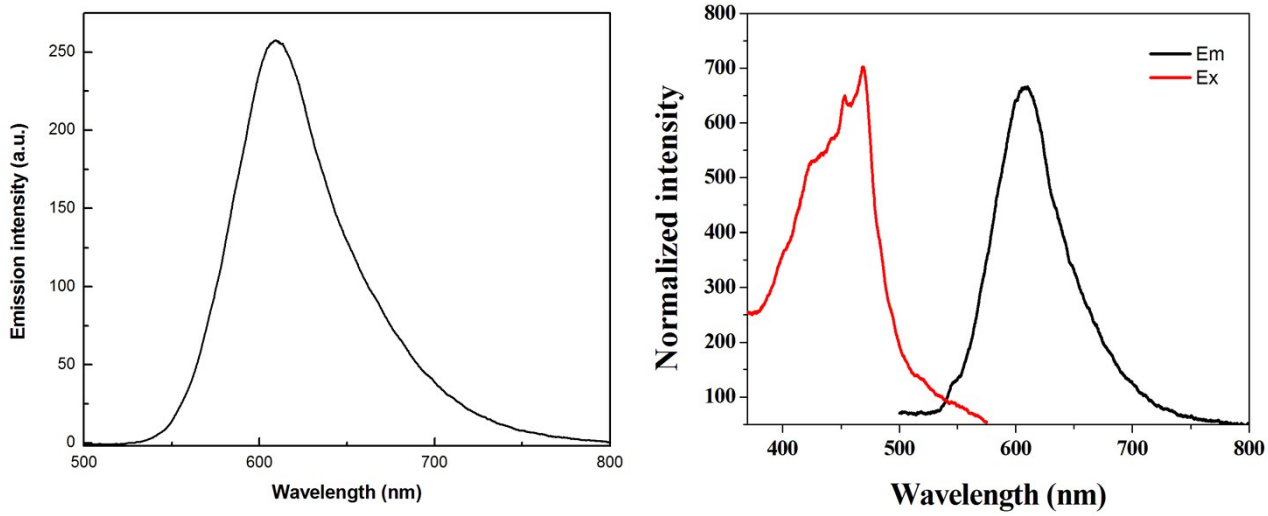

(a) (b)

Fig. S12 (a) The emission spectrum of the complex **1** obtained by excitation at 470 nm and recorded at ambient temperature in solvent (MeCN:EtOH = 1:19, 10^{-4} M); (b) Excitation and emission spectra for complex **1** at ambient temperature in solvent (MeCN:EtOH = 1:19, 10^{-4} M).

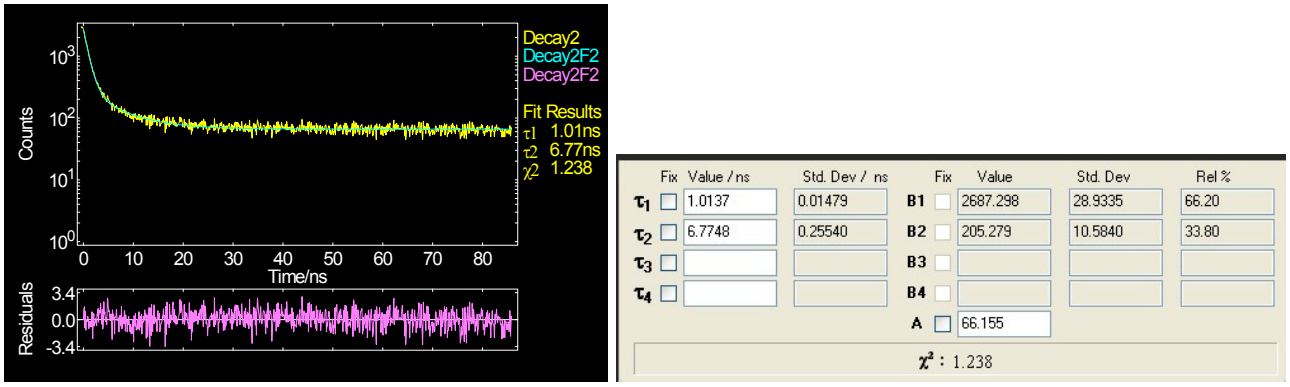

Fig. S13. Fluorescence decay curves, the corresponding fits and residuals plots of complex **1** in solid state.

The average lifetime of complex **1** was determined by allowing α_i and τ_i to vary, and then convoluting the following equation with the instrument response function.

$$I(t) = \sum_{i=1}^{n} a_i \exp(-t/\tau_i) \qquad (1)$$

The data of complex **1** was successfully modeled using double exponentials. The average lifetime was determined using the following equation:

$$\tau_{avg} = \frac{a_1\tau_1^{\,2} + a_2\tau_2^{\,2}}{a_1\tau_1 + a_2\tau_2} \qquad (2)$$

In both equations t is time, τ is lifetime, and α is a pre-exponential factor. (τ_1: 1.01 ns; α_1: 0.66; τ_2: 6.77 ns; α_2: 0.34).

Reference: G. Yuan, W. Shan, J. Chen, Y. Tian and H. Wang, *J. Lumin.*, 2015, **160**, 16-21.

Table S4. The lifetime of complex 1(10^{-4} M) in different solvents

Solvents	MeOH	EtOH	DCM	MeCN
τ, ns	194	202	319	155

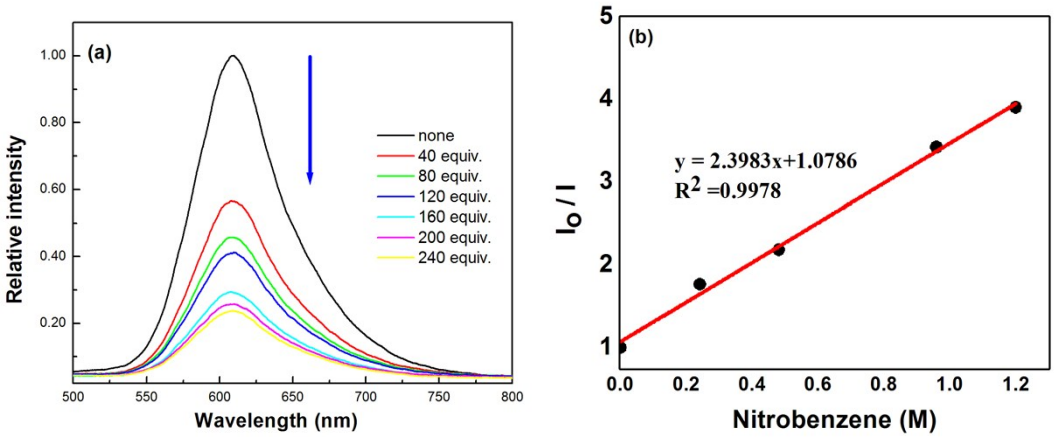

Fig. S14 (a) Quenching of complex **1** by 4-nitrobenzene (b) the Stern-Volmer plot for the quenching of complex **1** by 4-nitrobenzene.

Table S5. The lifetime of complex 1 at various quencher concentrations

Quencher equiv.	0	40	80	120	160	200	240
τ, ns	202	171.2	143.4	121.9	107.3	97.0	87.6

Fig. S15 **<u>The setup of photocatalytic devices</u>**

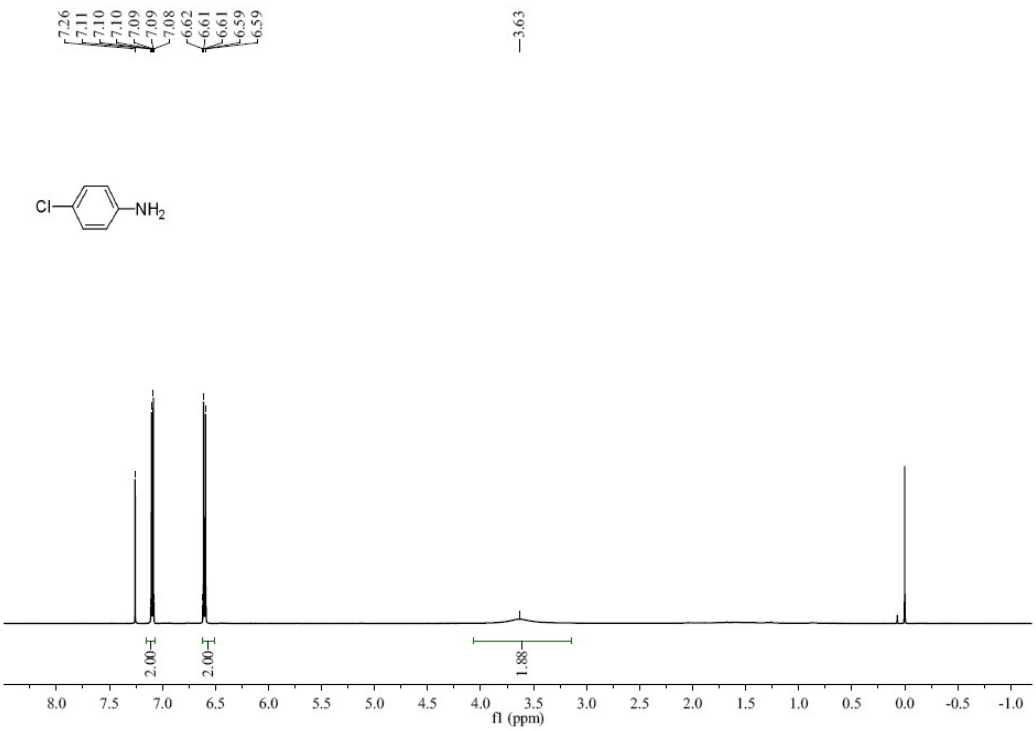

Figure S16. The ^{1}H NMR of 4-chloroaniline (400 MHz, $CDCl_3$)

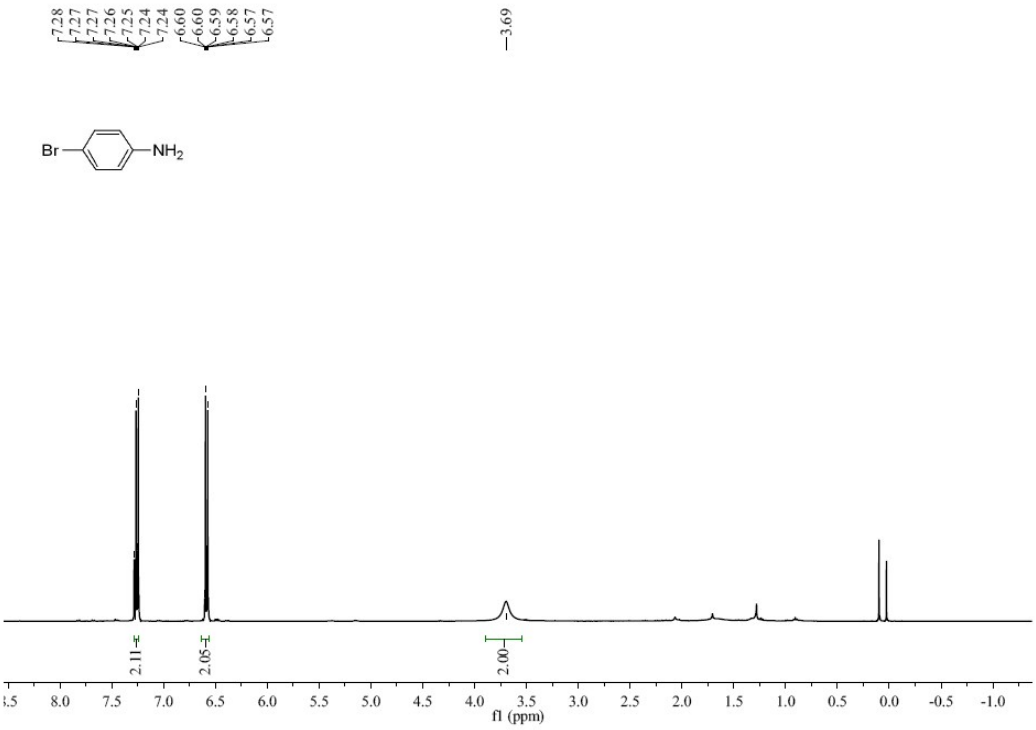

Figure S17. The ^{1}H NMR of 4-bromoaniline (400 MHz, $CDCl_3$)

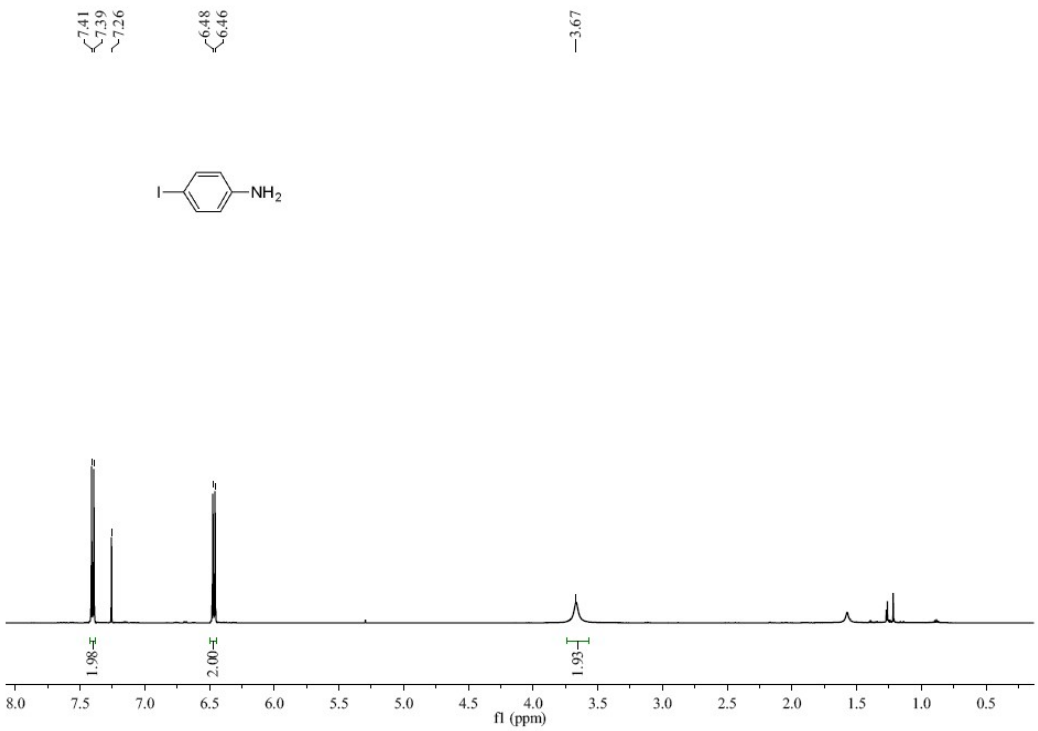

Figure S18. The ^{1}H NMR of 4-iodoaniline (400 MHz, $CDCl_3$)

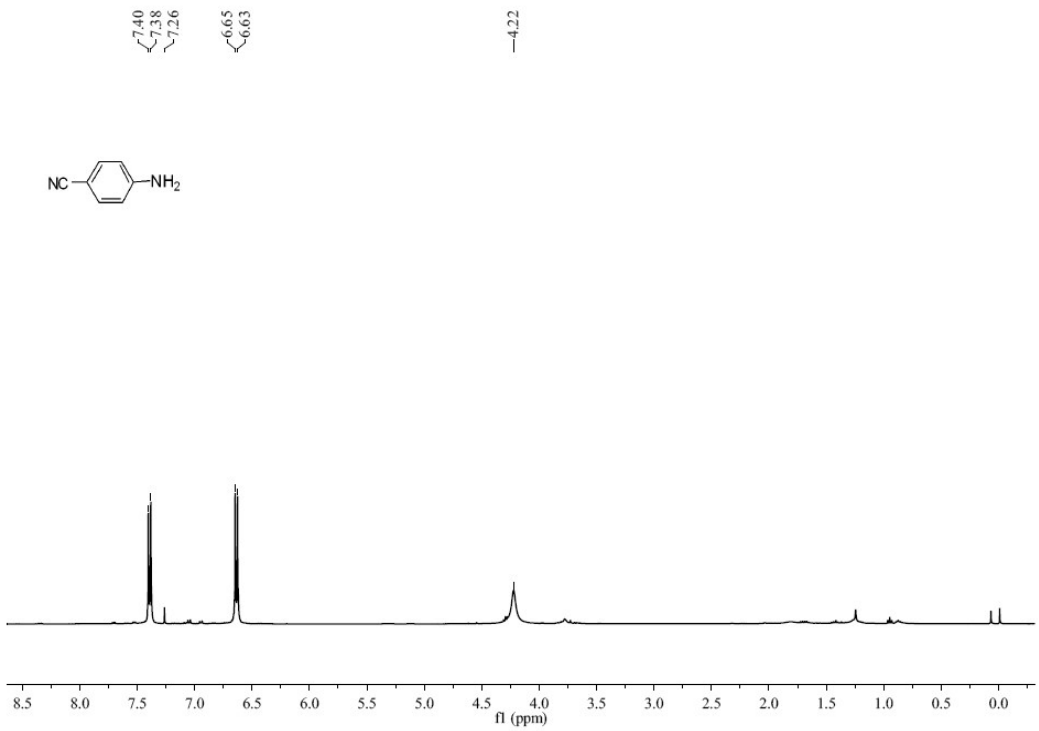

Figure S19. The ^{1}H NMR of 4-aminobenzonitrile (400 MHz, $CDCl_3$)

GC-yield Standard Curve

The response peak area ratios of product 4-chloroaniline and internal standard *n*-dodecane (**Ap/Ad**) were obtained from Agilent Thermo Trace1300 GC spectrometer. All the GC‐yields were calculated by the formula of curve fitting.

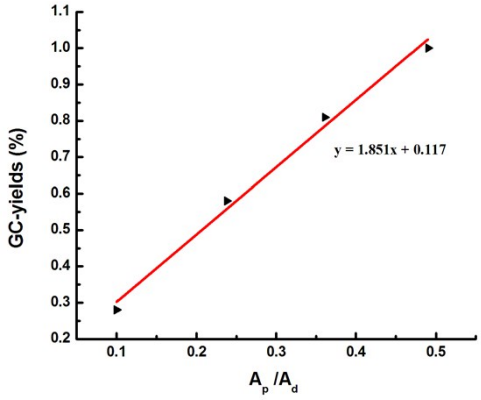

A_p/A_d	0.100	0.238	0.361	0.490
Yields	0.28	0.58	0.81	1.00

Figure S20. GC-Yield standard curve

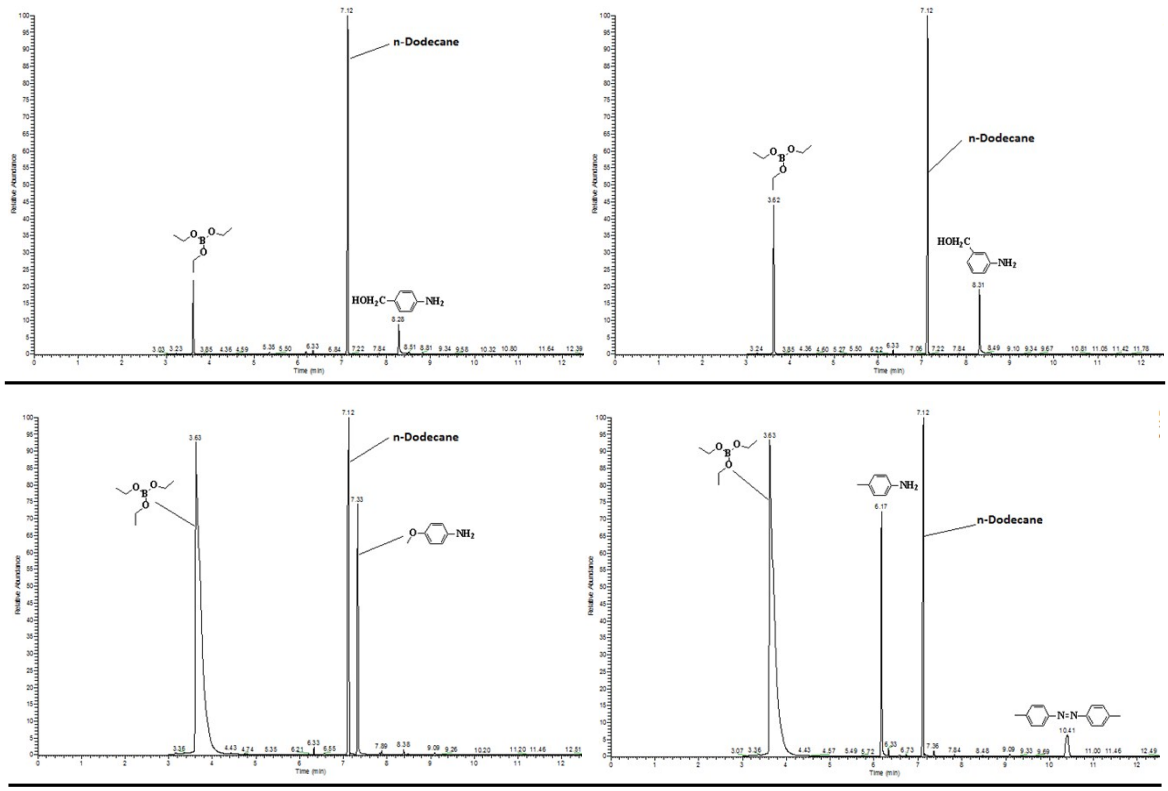

Fig. S21 **<u>The data of GC</u>**

Computational Methods

Density functional theory (DFT) calculations were carried out with Gaussian 16[1] computational chemistry suite. Geometries of gas phase minimum and transition state electronic structures were optimised using the Minnesota functional M06-L[2] with def2-SVP[3] basis set for all atoms. Frequency calculations were carried out at that level to ensure convergence, *i.e.* all positive eigenvalues for minima.

The time-dependent DFT (TD-DFT) calculations were carried out using the ORCA computational package (version 4.1.1)[4] with the same M06-L functional, triple zeta basis-set with RIJCOSX approximation[5-6] and Douglas-Kroll-Hess (DKH)[7-9] for scalar relativistic effects. The basis-set was defined as triple zeta TZVP[10] for Ru and def2-TZVP[11] for the rest of the atoms.

Due to the large molecular size of the photocatalysts, it is computationally demanding to optimize their corresponding excited state structures with TD-DFT. Instead, energy levels of the singlet S_1 and triplet excited states were TD-DFT single-point calculations based on geometries optimized in the singlet ground state S_0 structure. Thus the energy gaps for both compounds **Ru-1** and **Ru-bpy** in Scheme 1 of the manuscript were approximated as such.

From our calculations, the higher S_1 to triplet transition probabilities based on spin orbit coupling (SOC) calculations in **Ru-1** (compared to **Ru-bpy**) is consistent with experiment, for which we saw **Ru-1** exhibiting better photocatalytic properties. The SOC calculations were performed with ORCA using the quasi-degenerate perturbation theory (QDPT) framework.[12]

References

1. Frisch, M. J.; Trucks, G. W.; Schlegel, H. B.; Scuseria, G. E.; Robb, M. A.; Cheeseman, J. R.; Scalmani, G.; Barone, V.; Petersson, G. A.; Nakatsuji, H.; Li, X.; Caricato, M.; Marenich, A. V.; Bloino, J.; Janesko, B. G.; Gomperts, R.; Mennucci, B.; Hratchian, H. P.; Ortiz, J. V.; Izmaylov, A. F.; Sonnenberg, J. L.; Williams; Ding, F.; Lipparini, F.; Egidi, F.; Goings, J.; Peng, B.; Petrone, A.; Henderson, T.; Ranasinghe, D.; Zakrzewski, V. G.; Gao, J.; Rega, N.; Zheng, G.; Liang, W.; Hada, M.; Ehara, M.; Toyota, K.; Fukuda, R.; Hasegawa, J.; Ishida, M.; Nakajima, T.; Honda, Y.; Kitao, O.; Nakai, H.; Vreven, T.; Throssell, K.; Montgomery Jr., J. A.; Peralta, J. E.; Ogliaro, F.; Bearpark, M. J.; Heyd, J. J.; Brothers, E. N.; Kudin, K. N.; Staroverov, V. N.; Keith, T. A.; Kobayashi, R.; Normand, J.; Raghavachari, K.; Rendell, A. P.; Burant, J. C.; Iyengar, S. S.; Tomasi, J.; Cossi, M.; Millam, J. M.; Klene, M.; Adamo, C.; Cammi, R.; Ochterski, J. W.; Martin, R. L.; Morokuma, K.; Farkas, O.; Foresman, J. B.; Fox, D. J. *Gaussian 16 Rev. B.01*, Wallingford, CT, 2016.
2. Zhao, Y.; Truhlar, D. G., A new local density functional for main-group thermochemistry, transition metal bonding, thermochemical kinetics, and noncovalent interactions. *J. Chem. Phys.* **2006**, *125* (19), 194101.
3. Schäfer, A.; Horn, H.; Ahlrichs, R., Fully optimized contracted Gaussian basis sets for atoms Li to Kr. *J. Chem. Phys.* **1992**, *97* (4), 2571-2577.
4. Neese, F., Software update: the ORCA program system, version 4.0. *WIREs Comput. Mol. Sci.* **2018**, *8* (1), e1327.
5. Kossmann, S.; Neese, F., Comparison of two efficient approximate Hartee–Fock approaches. *Chem. Phys. Lett.* **2009**, *481* (4), 240-243.

6. Neese, F.; Wennmohs, F.; Hansen, A.; Becker, U., Efficient, approximate and parallel Hartree–Fock and hybrid DFT calculations. A 'chain-of-spheres' algorithm for the Hartree–Fock exchange. *Chem. Phys.* **2009**, *356* (1), 98-109.
7. Douglas, M.; Kroll, N. M., Quantum electrodynamical corrections to the fine structure of helium. *Ann. Physics* **1974**, *82* (1), 89-155.
8. Hess, B. A., Relativistic electronic-structure calculations employing a two-component no-pair formalism with external-field projection operators. *Phys. Rev. A* **1986**, *33* (6), 3742-3748.
9. Jansen, G.; Hess, B. A., Revision of the Douglas-Kroll transformation. *Phys. Rev. A* **1989**, *39* (11), 6016-6017.
10. Weigend, F.; Ahlrichs, R., Balanced basis sets of split valence, triple zeta valence and quadruple zeta valence quality for H to Rn: Design and assessment of accuracy. *Phys. Chem. Chem. Phys.* **2005**, *7* (18), 3297-3305.
11. Schäfer, A.; Huber, C.; Ahlrichs, R., Fully optimized contracted Gaussian basis sets of triple zeta valence quality for atoms Li to Kr. *J. Chem. Phys.* **1994**, *100* (8), 5829-5835.
12. Nesse, F, Efficient and accurate approximations to the molecular spin-orbit coupling operator and their use in molecular g-tensor calculations, *J. Chem. Phys.* **2005**, *122*, 034107.

XYZ coordinates

61
Ru-bpy

Ru	0.00115	0.00093	0.00073
N	-1.19765	-1.34495	-1.05018
C	-2.74869	-3.29440	-2.30635
C	-1.95953	-1.04092	-2.11678
C	-1.19718	-2.62589	-0.58435
C	-1.96752	-3.61472	-1.20288
C	-2.74387	-1.98043	-2.77183
H	-1.92781	-0.00189	-2.45299
H	-1.95694	-4.63512	-0.81997
H	-3.34074	-1.67958	-3.63326
H	-3.35328	-4.05930	-2.79572
N	-0.56877	1.71303	-1.04749
C	-1.48839	4.03028	-2.30029
C	-1.67886	2.35053	-0.57922
C	0.07258	2.22316	-2.11467
C	-0.35223	3.37180	-2.76818
C	-2.15333	3.51170	-1.19598
H	0.95693	1.67809	-2.45300
H	0.20439	3.73981	-3.63047
H	-3.04278	4.01050	-0.81121
H	-1.85135	4.93576	-2.78868
N	0.32571	-1.77427	1.04852
C	0.63383	-4.24825	2.30114
C	-0.34081	-2.86720	0.58023
C	1.13331	-1.91291	2.11593
C	1.31325	-3.12452	2.76919
C	-0.19846	-4.11343	1.19681
H	1.64662	-1.00984	2.45438
H	1.97831	-3.17968	3.63144
H	-0.73830	-4.97863	0.81218
H	0.75136	-5.21683	2.78918
N	1.37642	1.16827	1.04959
C	3.36349	2.67234	2.30388
C	1.09175	1.93702	2.11655
C	2.65639	1.13791	0.58184
C	3.66397	1.88414	1.19972
C	2.05016	2.69888	2.77069
H	0.05269	1.92943	2.45407
H	4.68345	1.84934	0.81589
H	1.76446	3.30266	3.63245
H	4.14313	3.25834	2.79268
N	1.76626	-0.36234	-1.05101
C	4.23031	-0.73158	-2.30641
C	1.88364	-1.17280	-2.11866
C	2.87580	0.27682	-0.58356
C	4.11749	0.10361	-1.20172
C	3.08956	-1.38271	-2.77335
H	0.96778	-1.66378	-2.45584
H	4.99635	0.62159	-0.81789
H	3.12727	-2.04888	-3.63565
H	5.19512	-0.87293	-2.79557
N	-1.69734	0.60460	1.05198
C	-3.99719	1.56546	2.30551
C	-2.21973	-0.02904	2.11788
C	-2.31391	1.72701	0.58514
C	-3.46599	2.22248	1.20248

C	-3.36058	0.41609	2.77145
H	-1.69200	-0.92430	2.45485
H	-3.94775	3.12195	0.81925
H	-3.73964	-0.13507	3.63245
H	-4.89602	1.94452	2.79398

81

Ru-1

Ru	0.07899	0.00247	0.00893
N	-1.52217	-0.60421	1.32104
C	-2.43140	-0.04190	2.37139
C	-3.55467	-1.10364	2.39134
O	-2.98125	-2.26906	1.74592
C	-1.90849	-1.82436	1.12610
H	-3.87644	-1.39662	3.39726
H	-4.44125	-0.81071	1.80821
N	-0.12705	-2.06190	-0.38798
C	0.63293	-3.17687	-1.05573
C	-0.46081	-4.25906	-1.10463
O	-1.37481	-3.90291	-0.03395
C	-1.12980	-2.63150	0.20541
H	-1.03637	-4.25131	-2.04395
H	-0.09864	-5.27580	-0.91697
C	1.76524	-3.59763	-0.12411
H	2.50330	-2.79490	0.00071
H	2.29293	-4.46381	-0.54624
H	1.39149	-3.88484	0.86898
C	1.16378	-2.81407	-2.42637
H	1.98380	-2.08780	-2.35791
H	0.38877	-2.40322	-3.08403
H	1.57212	-3.70916	-2.91476
C	-1.68138	-0.01061	3.69627
H	-2.31790	0.40923	4.48730
H	-0.78141	0.61471	3.62645
H	-1.38523	-1.02052	4.01525
C	-2.95093	1.33435	2.00290
H	-3.73214	1.64547	2.70979
H	-3.39096	1.35609	0.99626
H	-2.15334	2.08677	2.05360
N	-0.00485	2.09430	0.37373
C	0.76353	3.12453	1.14390
C	-0.09001	4.39132	0.88547
O	-0.96907	4.04365	-0.21384
C	-0.86372	2.74057	-0.34763
H	-0.72771	4.66805	1.73814
H	0.49260	5.26978	0.58424
N	-1.48041	0.69366	-1.32467
C	-1.67677	1.97235	-1.27249
O	-2.59761	2.51808	-2.03690
C	-3.04272	1.45246	-2.91213
C	-2.52342	0.15083	-2.25760
H	-2.60700	1.64147	-3.90498
H	-4.13425	1.51283	-2.99051
C	0.83767	2.78096	2.61867
H	1.37039	3.57092	3.16521
H	1.38707	1.84385	2.78275
H	-0.15997	2.68867	3.06807
C	2.15470	3.25802	0.53858
H	2.68512	4.10208	1.00015
H	2.11347	3.43991	-0.54505
H	2.75733	2.35949	0.72224
C	-3.62302	-0.53428	-1.45526
H	-4.03806	0.12735	-0.68216
H	-3.27204	-1.45915	-0.97901
H	-4.44841	-0.81795	-2.12265
C	-1.92954	-0.80360	-3.27208
H	-1.09402	-0.35715	-3.82780
H	-2.69141	-1.10299	-4.00456
H	-1.57391	-1.71688	-2.77824
N	1.68881	-0.44874	1.21245
C	3.98749	-1.07840	2.66770
C	2.92206	-0.29773	0.64982
C	1.60350	-0.94337	2.46097
C	2.72048	-1.26708	3.21866
C	4.08291	-0.59476	1.36829
H	0.59314	-1.07512	2.85093
H	2.59225	-1.66145	4.22715
H	5.06080	-0.45767	0.90611
H	4.88721	-1.31499	3.23745
N	1.66511	0.37100	-1.25594
C	3.93711	0.86306	-2.80273
C	1.55821	0.83206	-2.51543
C	2.90866	0.16676	-0.73566
C	4.05590	0.40014	-1.49767
C	2.66124	1.08873	-3.31799
H	0.54221	0.99058	-2.88165
H	5.04218	0.22582	-1.06699
H	2.51606	1.45975	-4.33302
H	4.82619	1.04998	-3.40662